Numerical Analysis of Airflow in Trachea Affected Thyroid Cancer Using Finite Volume Method

Arif Fatahillah*, Miftahul Jannah, Susi Setiawani, Toto Bara Setiawan, Arika Indah Kristiana

Mathematics Education, Faculty of Teacher Training and Education, University of Jember, Indonesia

Email: arif.fkip@unej.ac.id

ABSTRACT

Thyroid cancer is a cancer of the thyroid gland. In general, thyroid cancer causes stenosis of the trachea due to compression of the tracheal wall by the cancer. The purpose of this study is to analyze the velocity and pressure of airflow in the area of tracheal constriction due to thyroid cancer. This problem is solved using the finite volume method with SIMPLE (Semi Implicit Method for Pressure Linked Equation) discretization. This method is very suitable for discretizing irregularly shaped fluid flows. The software used is MATLAB and Ansys Fluent. MATLAB is used to compute numerical solutions and display graphs, while Fluent is used to visualize the airflow. The results show that as the percentage of stenosis increases, the airflow velocity increases while the pressure decreases, causing more severe respiratory distress. The results of this study can be a valuable reference for the treatment of patients with tracheal stenosis due to thyroid cancer.

Keywords: Thyroid cancer; Tracheal stenosis; Finite Volume Method; SIMPLE

INTRODUCTION

Mathematics serves as a fundamental and guiding science in the development of other sciences and its applicability spans various areas, including medicine. Medicine, as a scientific field, explores the means to maintain optimal human health and seeks to understand diseases and their treatment. Among the areas of study in medicine is the respiratory tract, a complex organ system that facilitates the exchange of oxygen and carbon dioxide. The respiratory system can be divided into two parts - the Upper Respiratory Tract and the Lower Respiratory Tract (LRT) [1]. The Upper Respiratory Tract comprises of the anterior nose, nasal passages, paranasal sinuses, nasopharynx, and oropharynx. Additionally, it includes a part of the larynx located above the vocal cords. On the other hand, the Lower Respiratory Tract covers part of the larynx situated beneath the vocal cords, trachea, small airways such as bronchi and bronchioles, as well as alveoli [1]. This study aims to examine the Lower Respiratory Tract with a special focus on the trachea.

The trachea, also known as the windpipe, is a flexible tube that measures 1.5 to 2 centimeters in diameter and 10 to 13 centimeters in length. It originates from the lower portion of the larynx and divides into two bronchi that lead to the lungs [2]. The tracheal wall is made up of 18 to 20 cartilage rings that have a D-shape, with the anterior and lateral walls composed of C-shaped cartilage, and a membranous posterior wall that connects the C-shaped cartilages [2], [3]. Each of these tracheal rings measures an average of 4 millimeters in height and 3 millimeters in wall thickness [3]. The trachea serves as a ventilation pathway, warming, humidifying, and purifying the air in the respiratory region while also protecting the airway from foreign objects through coughing [4].

The thyroid gland, located at the bottom of the neck in front of and beside the trachea and below the larynx [5], is a significant butterfly-shaped endocrine gland. Its key function is to regulate basal metabolic rate (BMR) and stimulate somatic and psychic growth [5]. As the largest endocrine gland, measuring around 2 inches and weighing between 15-25 grams, it is also the one most frequently affected by disease. Thyroid cancer is distinct from other cancers, as thyroid cells are the only ones in the human body capable of absorbing iodine [6]. Causes of this cancer typically include a history of goiter (enlarged thyroid), thyroid nodules, heredity, and exposure to radiation from medical treatments [7]. Based on its characteristics, thyroid cancer cases are predominant among women aged 50 to 54 [8], with papillary thyroid carcinoma being the most common type observed at Sanglah General Hospital in 2016 [6].

Thyroid cancer leads to the constriction of the airway, specifically the trachea, due to cancer cell pressure. Thyroid cancer leads to the constriction of the airway, specifically the trachea, due to cancer cell pressure. Thyroid cancer leads to the constriction of the airway, specifically the trachea, due to cancer cell pressure. The size of cancer cells correlates with the degree of constriction, ultimately resulting in tracheal stenosis. This medical condition, characterized by the narrowing of the upper trachea, can cause breathing issues, increased susceptibility to infection, and other related symptoms [9]. This stenosis trachea can lead to respiratory distress such as shortness of breath. Stenosis is categorized into Grade I-IV based on the reduction in the cross-sectional area of the trachea relative to the nominal area, ranging from $0 - 50\%$, $51 - 70\%$, $71 - 90\%$, and $> 91\%$ [9]. Each level of stenosis is associated with different symptomsngu [10]. Mild stenosis does not affect breathing stability, while moderate stenosis reduces breathing power, characterized by shortness of breath. In this condition, chemotherapy and drugs are necessary to shrink the cancer [10]. Severe to critical stenosis leads to a significant decrease in breathing capacity, resulting in breathing difficulties until death ensues. Surgical intervention in the form of ring installation is required to mitigate the condition [10]. According to a report in 2015, thyroid cancer is rapidly increasing in America, with an estimated 62,450 new cases and 1,950 deaths [7]. The annual mortality rate of thyroid cancer in Indonesia has increased by 36.4% since 1990, with 100,000 deaths reported each year [6], [11].

This study will model the airflow in the trachea due to thyroid cancer. The mathematical model used in this study is modified from Zobaer and Sutradhar's article where the model is formed using non-linear contact simulation between an ellipsoidal tumor and the trachea [12]. The study showed that as the tumor size increases, the diameter of the trachea shrinks, causing the airflow velocity to increase and resulting in a loss of respiratory power. Determination of the extent of narrowing was based on the level of tracheal narrowing where there are 4 levels of tracheal narrowing to identify the most appropriate surgical approach for the patient. The findings showed that surgery was necessary due to the sharp decrease in airflow that occurred at grade II, meaning the

stenosis ranged between 51% and 70% [9]. Another similar study modeled the airflow in the nasal cavity under normal and swollen conditions due to rhinitis and showed significant differences in airflow direction, temperature distribution, and relative humidity between the nasal cavity under normal and swollen walls [13]. In addition, there are studies related to the simulation of hot airflow in the upper and tracheal passages which showed that the upper and lower airways remained unaffected when the hot inlet temperature decreased [14]. When the temperature at the inlet increases, the burn damage intensifies and spreads to the nasal cavity and pharynx. As a result, the upper and lower airways become narrowed. Based on previous research, the novelty of this study is to model airflow in the trachea due to thyroid cancer affected by tracheal constriction, initial velocity, and initial pressure.

| Normal trachea based on CT scans [12] | Normal Trachea and Thyroid Cancer. | Tracheal stenosis model. |
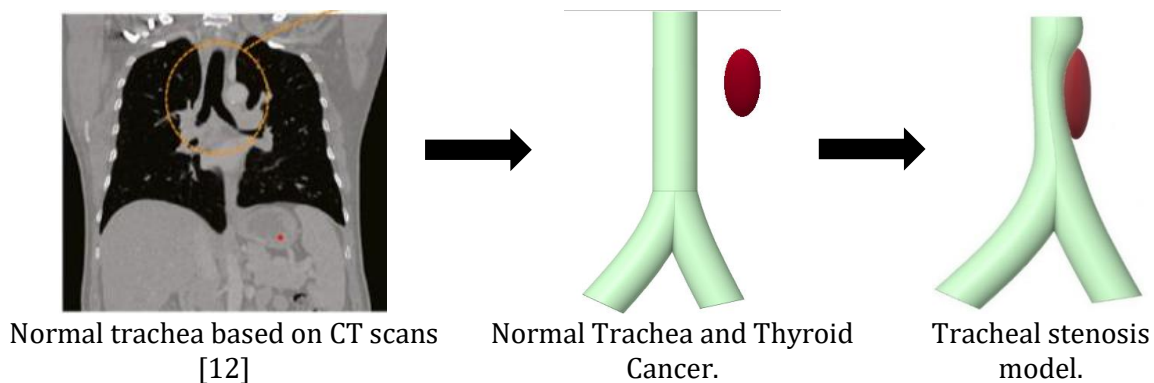
Figure 1. Tracheal constriction modeling flow in SpaceClaim

The finite volume method is a numerical approach that discretizes partial differential equations into discrete algebraic equations on a finite volume scale. It is widely used to discretize fluid flows with irregular shapes and is particularly suitable for numerical simulations involving fluid flow, heat, and mass transfer. It is widely used to discretize fluid flows with irregular shapes and is particularly suitable for numerical simulations involving fluid flow, heat, and mass transfer. It is widely used to discretize fluid flows with irregular shapes and is particularly suitable for numerical simulations involving fluid flow, heat, and mass transfer. The development of this method is closely related to advances in computational fluid dynamics (CFD) [15]. Computational Fluid Dynamics (CFD) is based on the fundamental physical principles of mass, momentum, and energy conservation [16], [17]. It is a branch of fluid mechanics that uses numerical methods and algorithms to solve problems related to fluid flow [18], [19]. Discretization is the mathematical process of converting continuous equations into discrete equations [16]. It is used to obtain approximate calculations or values that are close to the actual situation. The SIMPLE algorithm is a numerical method commonly used in computational fluid dynamics (CFD) to solve the fundamental equations of fluid mechanics [16]. It was developed by Prof. Brian Spalding and Suhas Patankar at Imperial College London in the early 1970s [20]. This study will solve the differential equation model [12] using the finite volume method with SIMPLE discretization technique. Additionally, simulations will be conducted using MATLAB and Ansys Fluent software programs. MATLAB is utilized for graph generation, while Ansys Fluent is employed for simulating airflow in the trachea. The mathematical model of momentum and mass equations [12] needs to be solved.

$$\frac{\partial \rho u}{\partial t} + \left[\frac{\partial \rho u}{\partial x} - \frac{\partial \rho u}{\partial x} \right] = 0 \tag{1}$$

$$\frac{\partial \rho u}{\partial t} + \left[u \frac{\partial \rho u}{\partial x} - u \frac{\partial \rho u}{\partial x} \right] = -\frac{\partial p}{\partial y} + \mu \frac{\partial^2 u}{\partial x^2} \tag{2}$$

with

$$p = \frac{128 \cdot v \cdot \mu \cdot l}{\pi \cdot d^4}$$

ρ represents the mass density, u refers to air flow velocity, p denotes pressure, μ stands for air viscosity, l represents trachea length, and d represents trachea diameter [12]. The aim of this research is to formulate and develop a mathematical model of air flow in the trachea caused by thyroid cancer. The mathematical model will be solved using the finite volume method and the SIMPLE discretization scheme. The model will be simulated with the assistance of the software Matlab and Fluent.

METHODS

The research methodology represents the process of obtaining data that will be analyzed until appropriate conclusions aligned with the research aim are reached. The research conducted follows a simulation research type. Simulation research is a form of research designed to obtain an overview through a simple system (model) by means of manipulation to achieve effects that approach reality. Simulation modeling is a method for combining various compatible models into a single comprehensive computer simulation that functions at full capacity [21]. This study will employ the finite volume method to mathematically model airflow in the trachea resulting from thyroid cancer. This study will employ the finite volume method to mathematically model airflow in the trachea resulting from thyroid cancer. The finite volume method is a numerical method used to solve mathematical models for irregular objects that is based on integral form and the principle of conservation [17]. The Volume Method requires fewer iteration time than the FEM method [22]. This method has a high accuracy value, facilitating the numerical simulation discretization process [23]. The discretization technique used in this study is the SIMPLE discretization method. SIMPLE (Semi-Implicit Method for Pressure Linked Equations) is a numerical method widely utilized for solving Navier-Stokes equations, which begins with determining initial guesses [24]. The fluid flow under investigation in this study is classified as unstructured gas. An algorithm was then created in MATLAB, and airflow geometry design in the trachea due to thyroid cancer was conducted using SpaceClaim. The next step involves calculating numerical values using the MATLAB program and simulating geometric design on Fluent. Fluent is a computer software utilized to conduct complicated fluid flow simulations. The final step is to analyze and draw conclusions from the simulation results.

RESULT AND DISCUSSION

Numerical analysis of airflow in the trachea due to thyroid cancer was performed by analyzing the numerical results of a mathematical model in MATLAB and geometric simulation in Fluent. Based on the findings of a scholarly study, variables affecting airflow in the trachea due to thyroid cancer were obtained. The following are the variables are used.

Table 1. Parameters with units [12]

No	Parameter	Unit value	Description
1	ρ	$1,225\ kg/m^3$	Air density
2	μ	$1,7894 \times 10^{-5} Ns/m^2$	Air viscosity
3	l	$0,08\ m$	Tracheal length
4	D	$0,02\ m$	Tracheal diameter
5	A_a	$0,0003142\ m^2$	Tracheal area

Using SIMPLE discretization, the simulation results are presented in a graphical table. The first case examines the impact of tracheal narrowing on the speed and pressure of airflow due to thyroid cancer. The stenosis degrees used were $25\%, 37.5\%, 50\%, 62.5\%$, and 75% with an initial velocity of $0,1\ m/s$, $0,2\ m/s$, $0,3\ m/s$ and an initial pressure of $110\ Pa$, $115\ Pa$, $120\ Pa$.

3.1 Analysis of Velocity Simulation Results

a. Graph of the effect stenosis

(a) $v_0 = 0,1\ m/s$ and $p_0 = 110\ Pa$ (b) $v_0 = 0,2\ m/s$ and $p_0 = 115\ Pa$

Figure 2. Effect of Stenosis Tracheal $(25\%, 37,5\%, 50\%, 62,5\%, 75\%)$
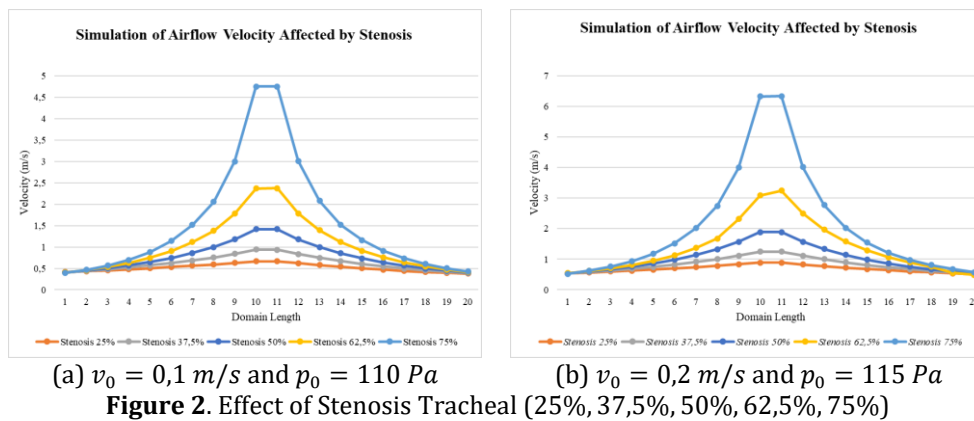
Figure 2 shows the simulation results of airflow velocity in the trachea affected by stenosis. The red, gray, dark blue, yellow, and light blue graphs show the airflow velocity with $25\%, 37.5\%, 50\%, 62.5\%$, and 75% stenosis, respectively. In Figure 2(a), the highest flow velocity is found at node 10, with the highest velocities being 0.6623 m/s, 0.9330 m/s, 1.4090 m/s, 2.3644 m/s, 4.7432 m/s respectively. This shows that when narrowing $25\%, 37.5\%$, and 50% airflow velocity is still stable, 62.5% is getting bigger, and 75% is very high in the narrowing area. Figure 2(b) also shows the highest flow velocity at 75% narrowing. So, it can be concluded that the greater the narrowing of the trachea, the greater the airflow velocity which results in reduced breathing power and the need for appropriate treatment.

b. Graph of the effect initial velocity

(a) Stenosis 25% and $P_0 = 110\ Pa$ (b) Stenosis 50% and $P_0 = 115\ Pa$

Figure 3.Effect of initial velocity
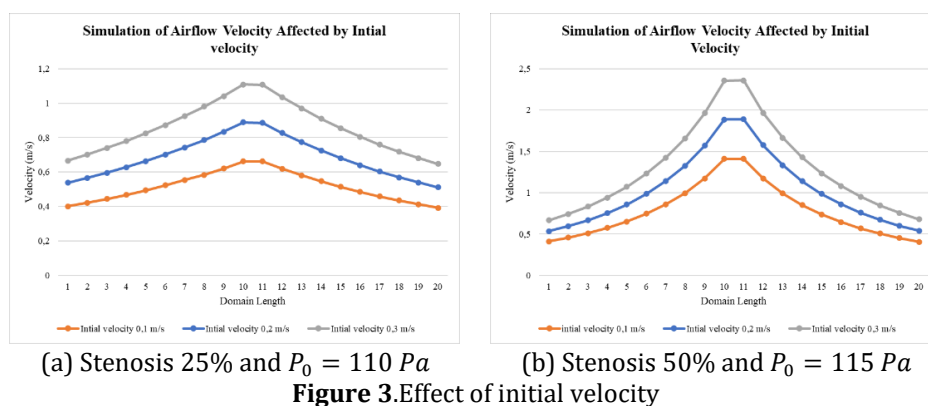
Figure 3 shows the simulation results of airflow velocity in the trachea as influenced by the initial velocity. The red, dark blue, and gray graphs show the airflow velocity with initial velocities of 0.1 m/s, 0.2 m/s, and 0.3 m/s, respectively. In Figure 3(a) the highest flow velocity is found at node 10, with each of the highest velocities being 0.7330 m/s, 0.8507 m/s, 1.1542 m/s. Figure 3(b) also shows that the highest flow velocity is when the initial velocity is 0.3 m/s. This shows that the greater the initial velocity, the greater the airflow velocity generated.

c. Fluent Simulation

Simulations were performed in 3 cases, namely to determine the pressure and velocity of airflow affected by tracheal constriction, air velocity, and initial pressure. Simulations were performed by designing five different images, the size of the constriction was 25%, 37.5%, 50%, 62.5%, and 75%. The simulated images were designed using SpaceClaim. The design of the tracheal constriction is shown in Figure 4.

(a) (b) (c) (d) (e)
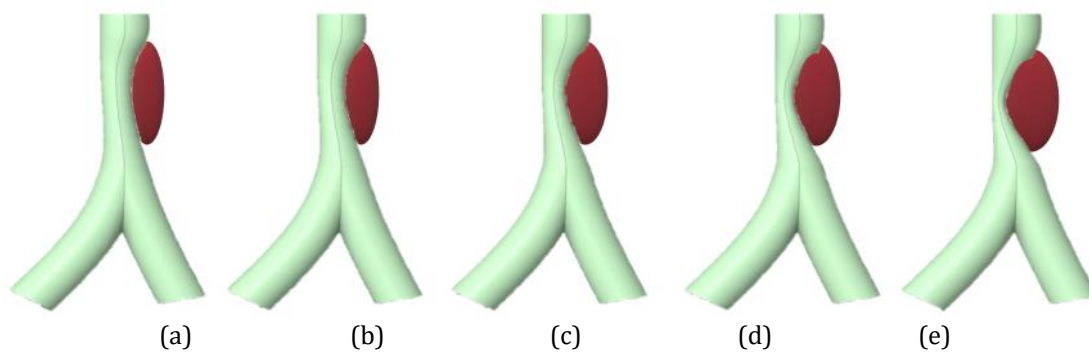
(a) Stenosis 25%; (b) Stenosis 37,5%; (c) Stenosis 50%; (d) Stenosis 62,5%; (e) Stenosis 75%

Figure 4. Design of tracheal constriction model

1. Airflow Velocity Simulation to Determine the Effect of Stenosis

(a) (b) (c) (d) (e)
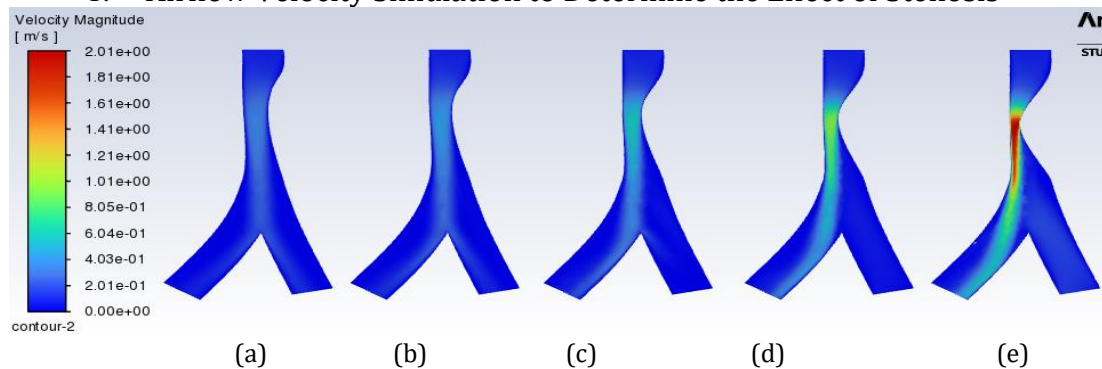
Figure 5. Plot vector airflow velocity affected by tracheal constriction

(a) Stenosis 25%; (b) Stenosis 37,5%; (c) Stenosis 50%; (d) Stenosis 62,5%; (e) Stenosis 75%

(a) (b) (c) (d) (e)
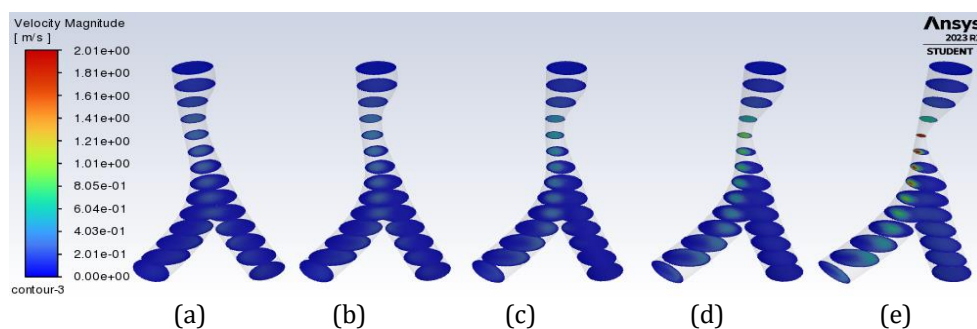
Figure 6. Airflow velocity plot in the form of slices affected by tracheal constriction

(a) *Stenosis* 25%; (b) Stenosis 37,5%; (c) Stenosis 50%; (d) Stenosis 62,5%; (e) Stenosis 75%

Figure 5 and Figure 6 present the results of air flow velocity simulation affected by tracheal constriction with an initial velocity of $0,1 \, m/s$. In Figure 5 and Figure 6, the contours of air flow velocity entering from both sides are shown in dark blue and change according to the constriction. Figure 5(a) and Figure 5(b) display light blue color, Figure 5(c) shows a gradient of light blue and green, Figure 5(d) indicates a gradient of light blue, green, and yellow, and Figure 5(e) presents a gradient of light blue, green, yellow, orange, and red upon entering the constricted region. This suggests that as the constriction increases, the air flow velocity also increases.

2. Airflow Velocity Simulation to Determine the Effect of Initial Velocity
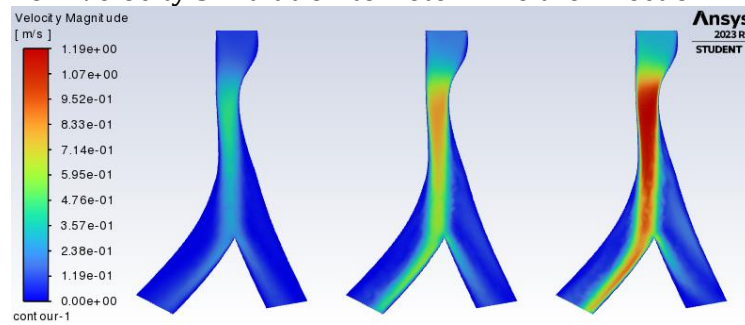
(a) $v_0 = 0,2 \, m/s$ (b) $v_0 = 0,4 \, m/s$ (c) $v_0 = 0,6 \, m/s$
Figure 7.Vector plot of airflow velocity as affected by initial velocity
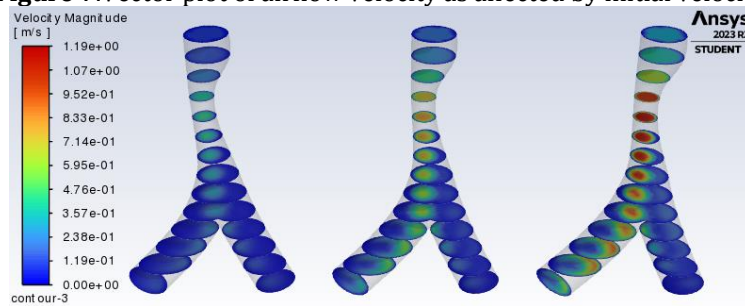
(a) $v_0 = 0,2 \, m/s$ (b) $v_0 = 0,4 \, m/s$ (c) $v_0 = 0,6 \, m/s$
Figure 8. Plot of airflow velocity in slices as affected by initial velocity

Figure 7 and Figure 8 present the results of air flow velocity simulations with a 37,5% constriction influenced by three different initial velocities such as $0,1 \, m/s$, $0,2 \, m/s$, and $0,3 \, m/s$. As shown in Figure 7 and Figure 8, the air velocity contours entering the constriction show a gradual shift from dark blue to light blue, and change according to the degree of constriction. Figure 7(a) displays a gradient of light blue and green colors, Figure 7(b) shows a gradient of light blue, green, yellow, and orange, and Figure 7(c) presents a gradient of light blue, green, yellow, orange, and red. This implies that as the initial velocity increases, the airflow velocity also increases.

3.2 Analysis of Pressure Simulation Results

a. Graph of the effect stenosis
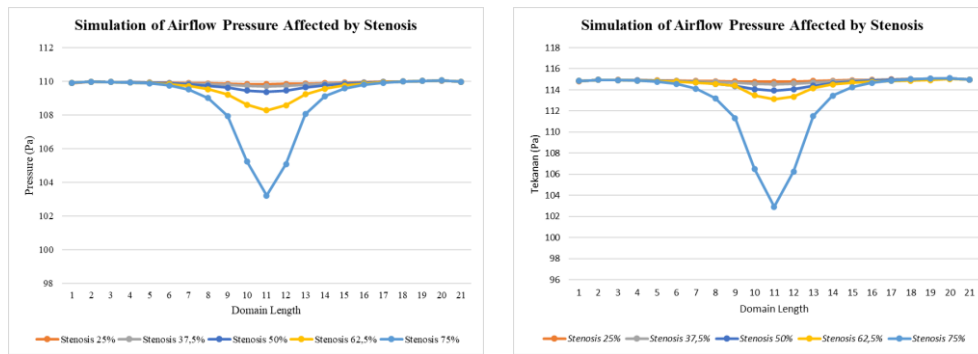
(a) $v_0 = 0,1 \ m/s$ and $p_0 = 110 \ Pa$ (b) $v_0 = 0,2 \ m/s$ and $p_0 = 115 \ Pa$

Figure 9. Effect of Stenosis Tracheal (25%, 37,5%, 50%, 62,5%, 75%)

Figure 9 shows the simulation results of airflow pressure in the stenosed trachea. The red, gray, dark blue, yellow, and light blue graphs show the airflow pressure with 25%, 37.5%, 50%, 62.5%, and 75% stenosis. In Figure 9(a) the lowest airflow pressure is when entering node 11, with the lowest airflow pressure values of $109,8330 \ Pa, 109,7088 \ Pa, 109,3733 \ Pa, \ 208,2746 \ Pa,$ and $\ 103,2089 \ Pa,$ respectively. In Figure 9(b) shows the lowest airflow pressure at 75% stenosis. It can be concluded that the greater the stenosed trachea, the lower the airflow pressure which results in reduced breathing power and the need for appropriate treatment.

b. Graph of the effect initial velocity
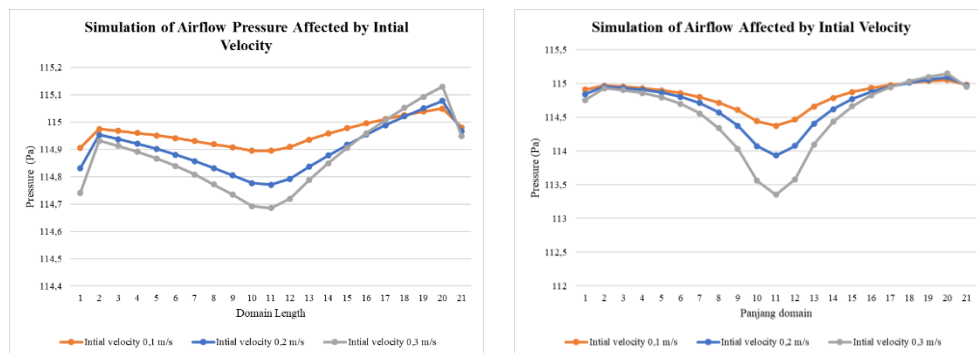
(a) Stenosis 25% and $P_0 = 110 \ Pa$ (b) Stenosis 50% and $P_0 = 115 \ Pa$

Figure 10. Effect of initial velocity

Figure 10 shows the simulation results of airflow pressure in the trachea as influenced by the initial velocity. The red, dark blue, and gray graphs show the airflow pressure with initial velocities of 0,1 m/s, 0,2 m/s, and 0,3 m/s, respectively. In Figure 10(a) the lowest flow pressure is found at node 11, with the lowest pressure being 114,8954 Pa, 114,7706 Pa, 114,6853 Pa respectively. Figure 10(b) also shows that the lowest airflow pressure is when the initial velocity is 0,3 m/s. This shows that the greater the initial velocity, the lower the airflow pressure.

c. Fluent Simulation

Simulations were performed in 3 cases, namely to determine the pressure and velocity of airflow affected by tracheal constriction, air velocity, and initial pressure. Simulations were performed by designing five different images, the size of the constriction was 25%, 37.5%, 50%, 62.5%, and 75%. The simulated images were designed using SpaceClaim. The design of the tracheal constriction is shown in Figure 4.

1. Airflow Pressure Simulation to Determine the Effect of Stenosis
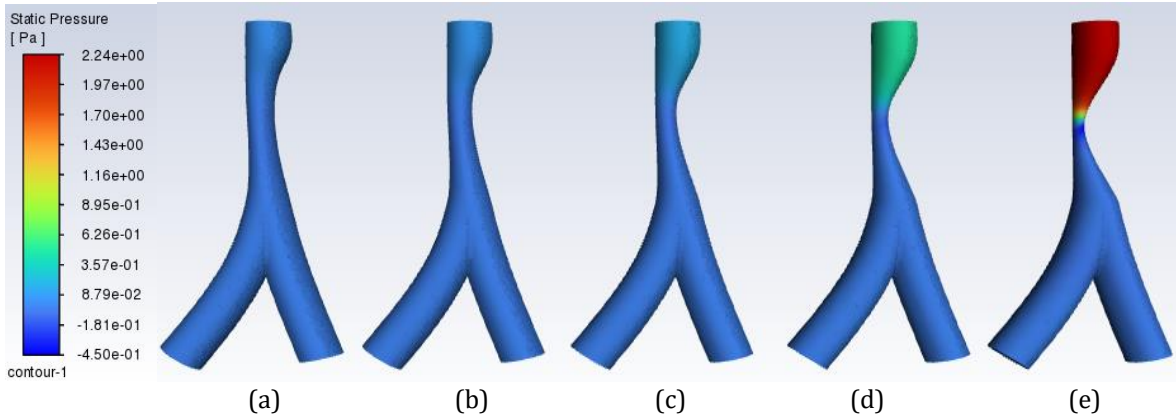
Figure 11. Simulated contours of airflow pressure affected by tracheal constriction
(a) Stenosis 25%; (b) Stenosis 37,5%; (c) Stenosis 50%; (d) Stenosis 62,5%; (e) Stenosis 75%

Figure 11 shows the results of a simulation of air flow pressure affected by stenosed trachea at an initial velocity of $0,1\ m/s$. The contour of the incoming air flow pressure is displayed in Figure 11, with different colors indicating varying degrees of pressure. Figure 11(a), Figure 11(b), and Figure 11(c) show light blue colors, while Figure 11(d) displays a gradient of green and light blue. Figure 11(e) reveals a gradient of colors including red, orange, yellow, green, and light blue upon entering the flow. When entering a narrowed area, the color changes to a dark blue. This indicates that the air flow pressure decreases as the stenosed becomes larger.

2. Airflow Velocity Simulation to Determine the Effect of Initial Pressure
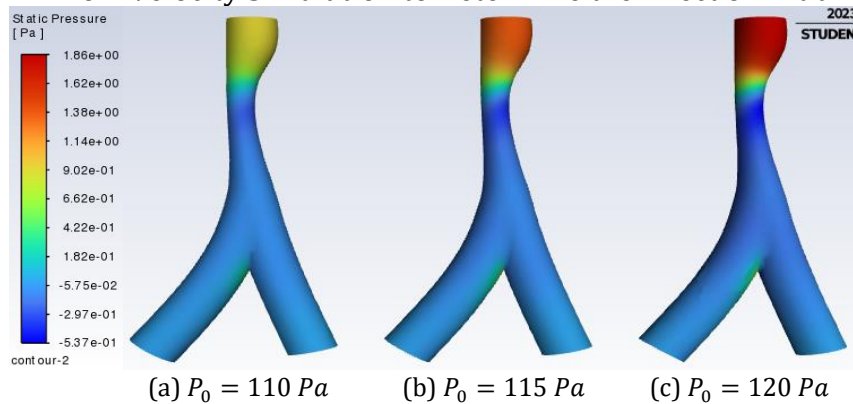
(a) $P_0 = 110\ Pa$ (b) $P_0 = 115\ Pa$ (c) $P_0 = 120\ Pa$
Figure 12. Simulated contours of airflow pressure as affected by initial pressure

Figure 12 illustrates the results of an air flow pressure simulation with a 37.5% constriction influenced by three different initial pressures: 110 Pa, 115 Pa, and 120 Pa. In each image of Figure 12, the colors of the air flow pressure represent different values. Figure 12(a) displays a color gradient of yellow, light green, and light blue. Figure 12(b) displays a color gradient of orange, yellow, light green, and light blue. Finally, Figure 12(c) displays a color gradient of red, yellow, light green, and light blue. As we enter the narrow section, the color of the third graph shifts to dark blue. This indicates that the initial pressure consistently decreases upon entering the constriction, and a steep decline occurs as the initial pressure increases.

Table 2. Potential loss of respiratory power due to tracheal constriction

	Stenosis	Velocity maximum
	25%	0,549236944
	37,5%	0,787874338
$v_0 = 0,1\ m/s$	50%	1,251590904
	62,5%	2,218237697
	75%	4,64724051
	25%	0.797586702
	37,5%	1.134679609
$v_0 = 0,2\ m/s$	50%	1.760423725
	62,5%	3.043997408
	75%	6.264674961
	25%	1.045489643
	37,5%	1.46705394
$v_0 = 0,3\ m/s$	50%	2.253547542
	62,5%	3.854954751
	75%	7.870181144

The simulation results show that all simulations have the potential to lose breathing power. The normal limit of respiratory airflow velocity is between $0,3\ m/s$ to $1\ m/s$.so if the highest airflow velocity exceeds the normal limit, it is prone to respiratory power loss. This can lead to shortness of breath and even respiratory arrest. Based on table, when the initial speed is $0,1\ m/s$ and the constriction is more than 50%, the airflow velocity exceeds the normal limit. Even when the intial speed rises the airflow velocity also rises, so the airflow velocity is getting binger. This means that when the constriction exceeds 50% and the intial velocity is $0,1\ m/s$, it is prone to loss of breathing power and needs treatment in the form of surgery or ring installation.

CONCLUSIONS

Based on the above discussion, a mathematical model of airflow in the trachea due to thyroid cancer is presented, which conveys equations of mass and momentum. Results from simulations conducted using Matlab and Ansys Fluent illustrate that as constriction increases, the velocity of airflow increases and the pressure of airflow decreases. The simulation results from both Matlab and Fluent indicate that an increase in initial respiratory air velocity leads to faster airflow and lower air pressure. The simulations also reveal that the respiratory impairment is most prone to occur when the constriction exceeds 50% and the initial velocity is above $0,1\ m/s$. This is due to the airflow velocity exceeding the normal limit, which falls between $0,3\ m/s$ and $1\ m/s$. Thus, it can be concluded that the higher the percentage of narrowing of the airflow passage, the higher the airflow velocity and the lower the airflow pressure, resulting in increased risk of respiratory impairment, such as shortness of breath. The Gauss-Seidel method yielded an error rate of less than $0,001$, and the effectiveness of the volume method was indicated by steadily decreasing residual values and converging iterations.

REFERENCES

[1] W. H. Man, W. A. A. de S. Piters, and D. Bogaert, "The Microbiota of the Respiratory Tract: Gatekeeper to Respiratory Health," *Nature Reviews Microbiology*, vol. 15, no. 5. Nature Publishing Group, pp. 259–270, Apr. 10, 2017. doi: 10.1038/nrmicro.2017.14.

[2]   B. E. M. Brand-Saberi and T. Schäfer, "Trachea: Anatomy and physiology," *Thoracic Surgery Clinics*, vol. 24, no. 1. pp. 1–5, Feb. 2014. doi: 10.1016/j.thorsurg.2013.09.004.

[3]   P. W. Furlow and D. J. Mathisen, "Surgical anatomy of the trachea," *Ann Cardiothorac Surg*, vol. 7, no. 2, pp. 255–260, Mar. 2018, doi: 10.21037/acs.2018.03.01.

[4]   S. Haykal, M. Salna, T. K. Waddell, and S. O. Hofer, "Advances in Tracheal Reconstruction," *Plastic and Reconstructive Surgery*, vol. 2, no. 7. Lippincott Williams and Wilkins, Jul. 09, 2014. doi: 10.1097/GOX.0000000000000097.

[5]   Y. Khan and A. Farhan, *Histology, Thyroid Gland*. Treasure Island (FL): Stat Pearls, 2019.

[6]   K. Arrumugam, N. P. Ekawati, and I. M. Gotra, "Characteristic of Thyroid Carcinoma based on Age, Sex and Histology Type at Sanglah General Hospital, Bali, Indonesia, 2016," *DiscoverSys*, vol. 9, no. 3, pp. 124–126, 2018, doi: 10.1556/ism.v9i3.285.

[7]   "Cancer Facts & Figures 2015," Atlanta, 2015.

[8]   M. E. Cabanillas, D. G. McFadden, and C. Durante, "Thyroid cancer," *The Lancet*, vol. 388, no. 10061. Lancet Publishing Group, pp. 2783–2795, May 2016. doi: 10.1016/S0140-6736(16)30172-6.

[9]   W. J. Poynot, K. A. Gonthier, M. E. Dunham, and T. W. Crosby, "Classification of Tracheal Stenosis in Children based on Computational Aerodynamics," *J Biomech*, vol. 104, pp. 1–11, May 2020, doi: 10.1016/j.jbiomech.2020.109752.

[10]   Q. T. Nguyen *et al.*, "Diagnosis and Treatment of Patients with Thyroid Cancer," vol. 8, no. 1, pp. 30–40, 2015, [Online]. Available: www.AHDBonline.com

[11]   G. Pellegriti, F. Frasca, C. Regalbuto, S. Squatrito, and R. Vigneri, "Worldwide increasing incidence of thyroid cancer: Update on epidemiology and risk factors," *Journal of Cancer Epidemiology*, vol. 2013. 2013. doi: 10.1155/2013/965212.

[12]   T. Zobaer and A. Sutradhar, "Modeling the effect of tumor compression on airflow dynamics in trachea using contact simulation and CFD analysis," *Comput Biol Med*, vol. 135, Aug. 2021, doi: 10.1016/j.compbiomed.2021.104574.

[13]   A. Issakhov, A. Mardieyeva, Y. Zhandaulet, and A. Abylkassymova, "Numerical study of air flow in the human respiratory system with rhinitis," *Case Studies in Thermal Engineering*, vol. 26, Aug. 2021, doi: 10.1016/j.csite.2021.101079.

[14]   H. Shamohammadi, S. Mehrabi, S. Sadrizadeh, M. Yaghoubi, and O. Abouali, "3D numerical simulation of hot airflow in the human nasal cavity and trachea," *Comput Biol Med*, vol. 147, Aug. 2022, doi: 10.1016/j.compbiomed.2022.105702.

[15]   F. Moukalled, L. Mangani, and M. Darwish, "Fluid Mechanics and Its Applications The Finite Volume Method in Computational Fluid Dynamics." [Online]. Available: http://www.springer.com/series/5980

[16]   H. Khawaja and M. Moatamedi, "Semi-Implicit Method for Pressure-Linked Equations (SIMPLE) - solution in MATLAB®," 2018.

[17]   M. M. Bhatti, M. Marin, A. Zeeshan, and S. I. Abdelsalam, "Editorial: Recent Trends in Computational Fluid Dynamics, 2nd Edition," *Mathematical and Statistical Physics*, 2020, doi: 10.3389/978-2-88966-900-4.

[18]   Y. Zhao and X. Su, *Computational Fluid-Structure Interaction: Methods, Models, and Applications*. Chennai: Matthew Deans, 2019. doi: https://doi.org/10.1016/11978-0-12-814770-2.000001-6.

[19]   P. D. Dwidmuthe, G. G. Dastane, C. S. Mathpati, and J. B. Joshi, "Study of blood flow in stenosed artery model using computational fluid dynamics and response surface methodology," *Can J Chem Eng*, vol. 99, no. S1, pp. S820–S837, Oct. 2020, doi: 10.1002/cjce.23991.

[20] J. H. Kao and P. Y. Tseng, "Application of Computational Fluid Dynamics (CFD) Simulation in a Vertical Axis Wind Turbine (VAWT) System," in *IOP Conference Series: Earth and Environmental Science*, Institute of Physics Publishing, Feb. 2018. doi: 10.1088/1755-1315/114/1/012002.

[21] J. M. Durán, "What is a Simulation Model?," *Minds Mach (Dordr)*, vol. 30, no. 3, pp. 301–323, Sep. 2020, doi: 10.1007/s11023-020-09520-z.

[22] J. Wang, Y. Wang, and J. Shi, "On Efficiency and Effectiveness of Finite Volume Method for Thermal Analysis of Selective Laser Melting," *Engineering Computations (Swansea, Wales)*, vol. 37, no. 6, pp. 2155–2175, May 2020, doi: 10.1108/EC-03-2019-0106.

[23] Y. Zhao, Y. Kim, M. S. Hossain, M. Nazem, J. Liu, and Y. Hu, "Numerical advancements on the analysis of dynamically installed anchors," *Ocean Engineering*, vol. 182. Elsevier Ltd, pp. 343–359, Jun. 15, 2019. doi: 10.1016/j.oceaneng.2019.04.079.

[24] H. K. Versteeg and W. Malalasekera, *An Introduction to Computational Fluid Dynamics Second Edition*, 2nd ed. 2007. [Online]. Available: www.pearsoned.co.uk/versteeg